Journal of Nuclear Materials 383 (2008) 97–111

Contents lists available at ScienceDirect

Journal of Nuclear Materials

journal homepage: www.elsevier.com/locate/jnucmat

IGSCC of non-sensitized stainless steels in high temperature water

Peter L. Andresen *, Martin M. Morra

GE Global Research Center, One Research Circle, CE 2513, Schenectady, NY 12309, United States

ARTICLE INFO

PACS:
82.45.Bb
81.40.Np

ABSTRACT

SCC studies in stainless steels and nickel alloys reveal that all grades and conditions are susceptible to SCC in high temperature water, whether deaerated or aerated, high H_2 or low, theoretical purity water or buffered/contaminated, lower temperature or higher. However, the kinetics of SCC growth vary enormously with stress intensity, yield strength, sensitization, water chemistry, irradiation, temperature, etc. The role of yield strength is especially important because it changes with surface cold work, bulk cold work, weld shrinkage strain, and irradiation hardening; the role of metallurgical strengthening mechanisms, e.g., nitrogen additions or precipitation hardening, may have a similar effect. SCC growth rate measurements were performed in high temperature water on unsensitized stainless steels (and alloy 600) of various grades and compositions. Little effect of grade/heat of stainless steel, martensite content or H_2 fugacity/permeation rate was observed, while large effects were observed for yield strength (cold work), stress intensity factor, corrosion potential, and temperature. A model 'stainless steel' containing 5% Si (and elevated Ni and reduced Cr) showed high growth rates and little effect of corrosion potential or stress intensity factor.

1. Introduction

Stress corrosion cracking (SCC) in stainless steels and nickel alloys has occurred in various unirradiated and irradiated components in light water reactors. Despite many observations and common characteristics, SCC is often compartmentalized into small, unique modes with individualized mechanisms and dependencies [1–7]. It is now acknowledged [1–8] that the crack tip is deaerated and at low potential in all cases, the environmental conditions under which crack advance occurs in light water reactor systems are very similar [1,2,4–7]. Primary differences are associated with: coolant additives that shift the pH at temperature from 5.6 to ≈7.0; H_2 fugacity (≈50 vs. 3000 ppb H_2); and temperature (274 °C vs. 323 °C – or higher in the pressurizer). Of these differentiating factors, temperature is the most important in stainless steels; temperature and H_2 are both important in nickel alloys. B/Li or NH_3 in the pH_T range ~5.5–8.0 has little effect on SCC growth rates in deareated water, unlike their effect in aerated water [9]. The existence of surface cold work, weld shrinkage strains, bulk cold work and irradiation hardening elevate the importance of understanding the mechanism and kinetics associated with cold work or, more fundamentally, yield strength. Cold work increases the SCC growth rate under all conditions – high and low corrosion potential, temperature, sensitization, stress intensity factor, etc.

2. Experimental procedures

Stainless steels were typically solution annealed at 1050 °C (1100 °C for alloy 600) for 30 min followed by a water quench. Deformation was typically introduced by heating the plate material to +140 °C (or cooling to −55 °C; alloy 600 was rolled at 25 °C) and rolling about half of the total reduction in each direction. Rolling at +140 °C (termed 'cool work' in this paper) produces much less deformation-induced martensite in these stainless steels than rolling at −55 °C (termed 'cold work'). Some materials were worked by forging. No deformation-induced martensite forms in alloy 600. Martensite content was evaluated by optical metallography following etching or ferrofluid staining.

0.5T compact type for cold worked materials (and 1T compact type for the annealed materials) were machined with 5% side grooves on each side. CT specimens were instrumented with platinum current and potential probe leads for dc potential drop measurements of crack length. In this technique, current flow through the sample is reversed about once per second primarily to reduce measurement errors associated with thermocouple effects and amplifier offsets. The computer control of current reversal, data acquisition, data averaging techniques, the relationship between measured potential and crack length, and control of constant stress intensity factor have been presented previously [10–13]. Data were stored in a permanent disk file typically once every 1.5 h. In addition to the data record number, total elapsed and incremental time, and crack length, the system measured and stored the temperature, current, corrosion potential, dissolved gases, influent and

* Corresponding author.
E-mail address: andresen@crd.ge.com (P.L. Andresen).

0022-3115/$ - see front matter © 2008 Elsevier B.V. All rights reserved.
doi:10.1016/j.jnucmat.2008.08.005

effluent conductivity, load and time/date. Additionally, both operator and automated program messages describing changes in test conditions and test status were a permanent part of the data record.

Zirconia sleeves were used to electrically isolate most CT specimens from the loading pins using, and within the autoclave a zirconia washer also isolated the upper pull rod from the internal load frame. The lower pull rod was electrically isolated from the autoclave using an Omniseal pressure seal and from the loading actuator using an insulating washer. Ground isolated instrumentation was used for the platinum current and potential probe attachments to the specimen.

Crack extension from the machined notch by 0.5–2.0 mm was performed typically at 1 Hz at a load ratio (K_{min}/K_{max}) $R = 0.5$, 0.6 and 0.7 and at a K_{max} somewhat below the test value of about 27.5 MPa$\sqrt{m}$. Subsequent pre-cracking in the environment to transition the crack morphology and plastic zone characteristics was performed at decreasing frequency to 0.001 Hz, then by introducing a hold time at K_{max} (while maintaining $R = 0.7$), and finally by switching to fully static load. Testing was performed using Instron Model 1362 servo-electric testing machines, Instron Model 1350 servo-hydraulic machines equipped with a single stage, low flow servovalve to ensure optimal (non-noisy) response, or Interactive Instruments Models 2K-16 or 4K-16 controllers. All systems were equipped with digital controls that provide improved machine control and full computer interface/control capabilities, including constant K control, K rising/falling profiles, and multi-condition tables that permit different K/R/frequency/hold time conditions to be sequentially evaluated. Constant K control was employed in most tests, with load corrections applied after very small increases in stress intensity, typically <0.1%. To avoid 'hunting' (increases and decreases in load), decreases in crack length never produced load corrections.

SCC growth rates can be considered statistically meaningful when the crack growth increment is at least 10 times the resolution of the technique, which was typically 0.001–0.005 mm. Thus, crack length increments were typically >0.05 mm, although for very low growth rate conditions, smaller increments were occasionally used to reduce testing time from several months per datum to several weeks. The correlation coefficients from linear

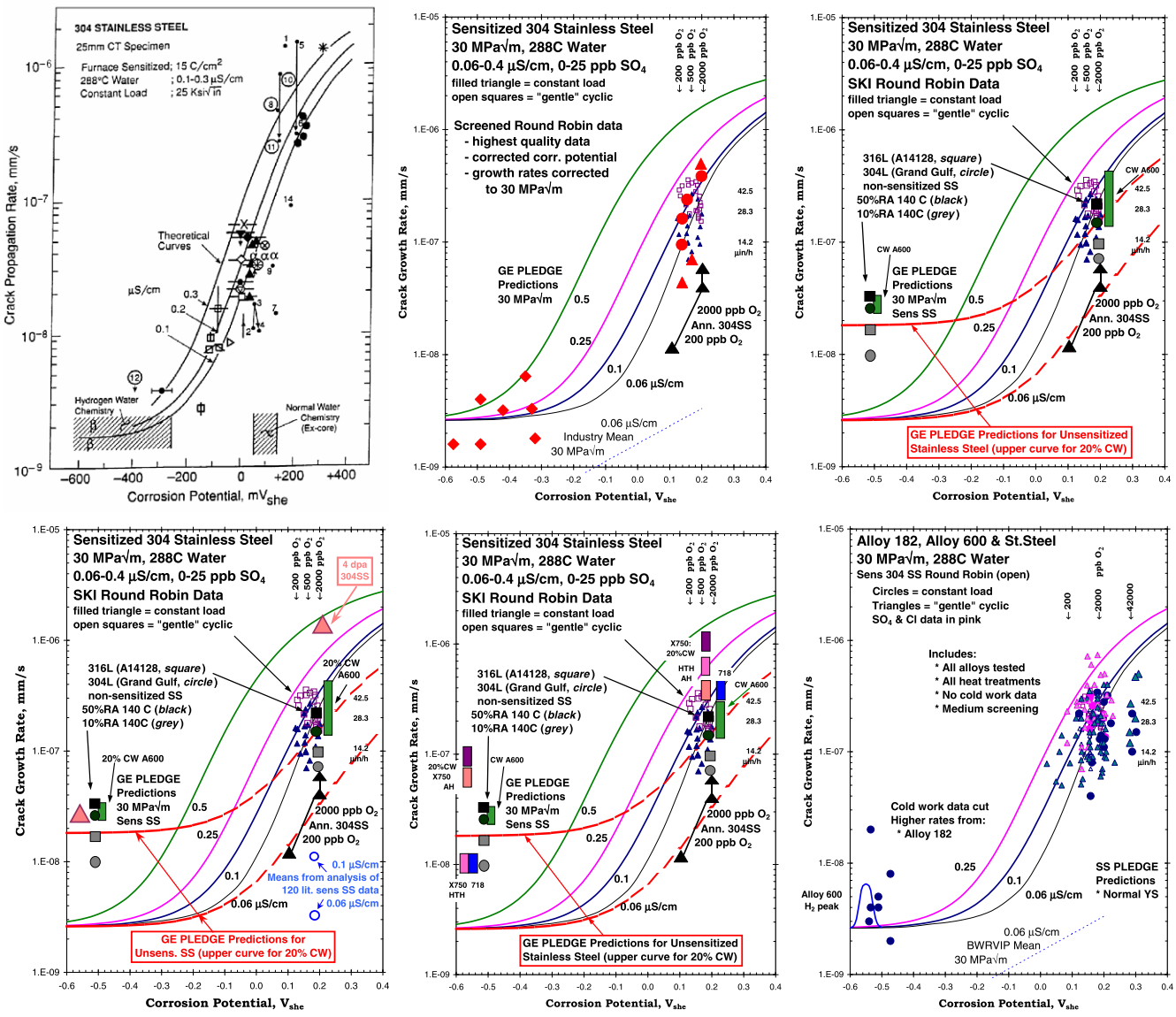

Fig. 1. SCC growth rate vs. corrosion potential in 288 °C high purity water for stainless steel (upper graphs) and also for irradiated stainless steel (lower left) and nickel alloys (two at lower right).

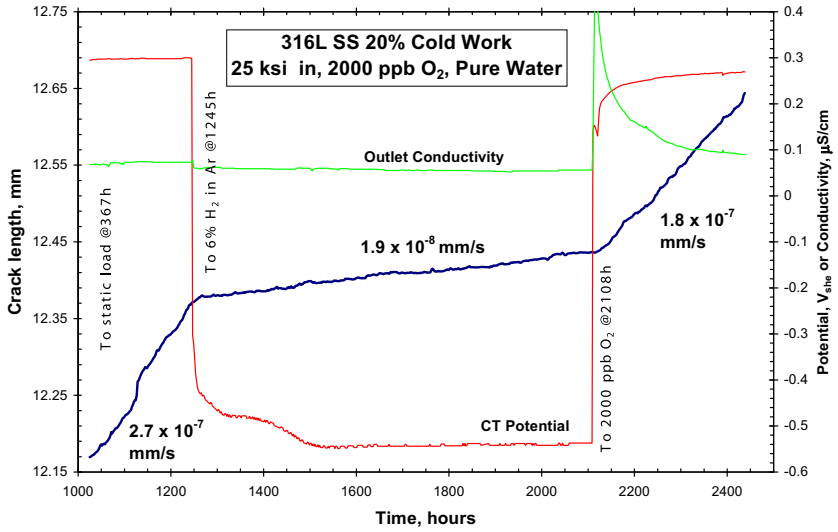

Fig. 2. Crack length vs. time for a 0.5TCT specimen of unsensitized Type 316L stainless steel 'cold' worked at −55 °C to 20% reduction in area.

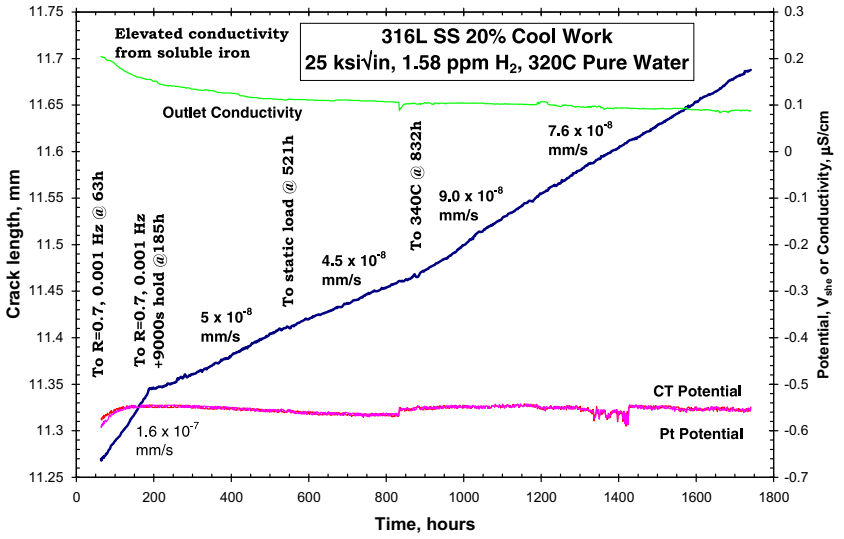

Fig. 3. Crack length vs. time for a 0.5TCT specimen of unsensitized Type 316L stainless steel 'cool' worked at +140 °C to 20% reduction in area.

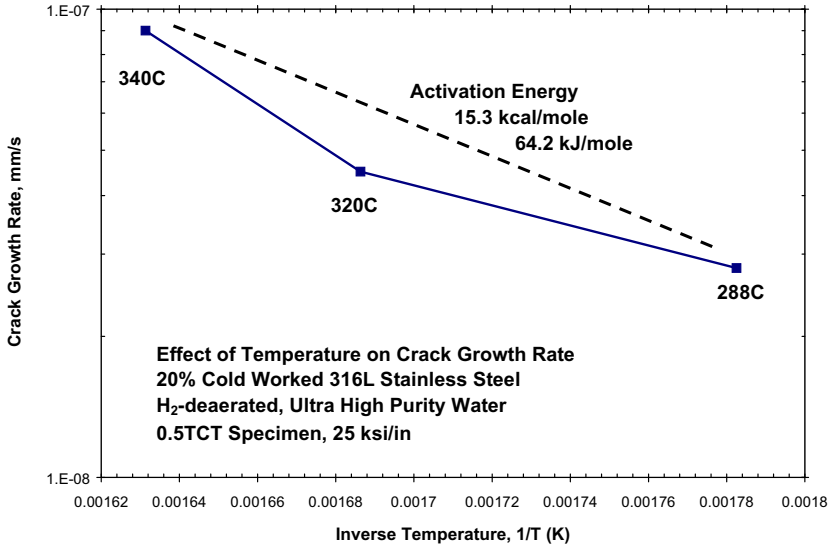

Fig. 4. Activation energy for SCC of Type 316L stainless steel in pure water.

regression analyses of the crack lengths vs. time data from which growth rates are calculated were typically >0.98. The dc potential drop technique is typically close to the actual incremental crack depth (generally within 10–20%, although if the crack front is very uneven, larger errors are inevitable).

Deaerated, demineralized water was drawn through another demineralizer and submicron filter to ensure ultra high purity (0.055 μS/cm) and then into a glass column (6.4-cm diameter by 183 cm long). A low pressure pump provided positive pressure to the high pressure pump, and drew water from and recirculated excess water (water that did not go into the high pressure pump) back into the glass column. The autoclave effluent was back-pressure regulated, then measured for conductivity using a Sybron Barnstead Model PM-512 and dissolved oxygen using an Orbisphere Model 2606. The oxygen concentration was controlled by bubbling gas mixtures blended by a Tylan Model RO-20-A mass flow controller. Impurities were added to the glass column using a metering pump (Fluid Metering Model RP-G50/H1 GKC) which was controlled by the Sybron Barnstead conductivity meter. Tests were performed in 4 liter stainless steel autoclaves at 288 °C and 10.3 MPa (1500 psi). Corrosion potential of the CT specimen and a Pt coupon were measured using a zirconia membrane reference electrode [14].

3. Results and discussion

The historical concepts of immunity and thresholds to SCC have largely given way as more sophisticated measurement techniques have been employed [15–17]. For example, the absence of thresholds for sensitization, corrosion potential, and water purity are evident in Fig. 1, which shows data (and predictions) for sensitized and unsensitized stainless steel in moderate to high purity

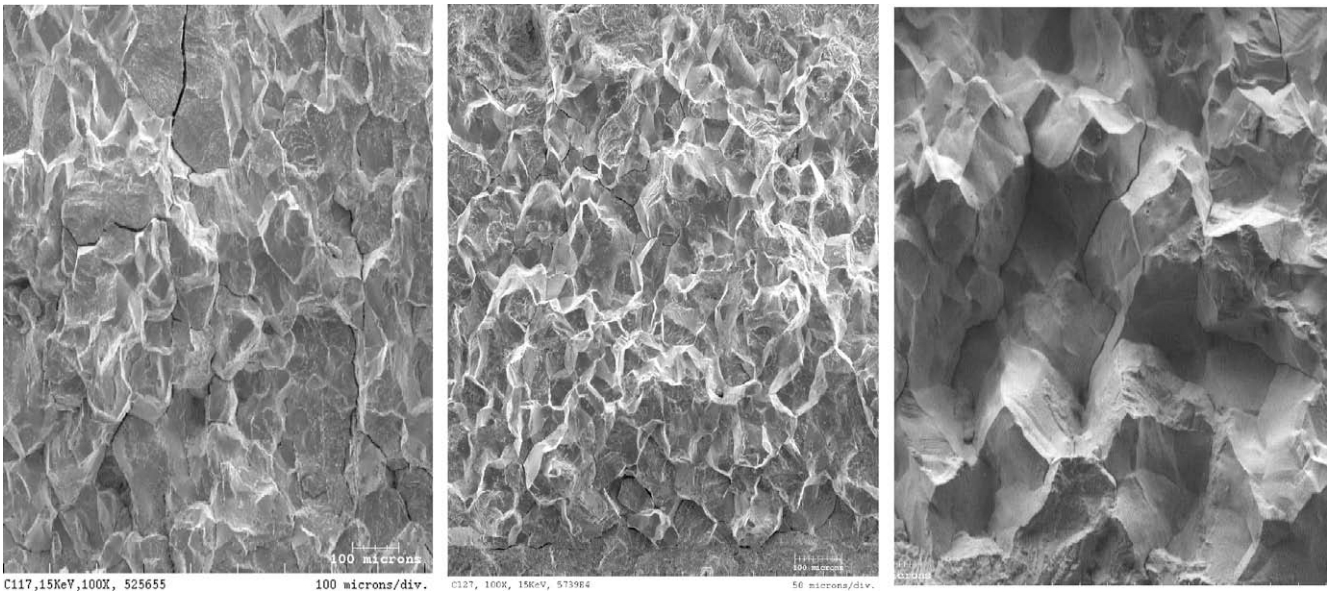

Fig. 5. Intergranular SCC morphology. Top left: 20% CW (−55 °C) Type 304L SS. Top right: 20% CW Type 316L SS. Bottom left: 20% CW alloy 600. Bottom right: alloy 182 weld metal.

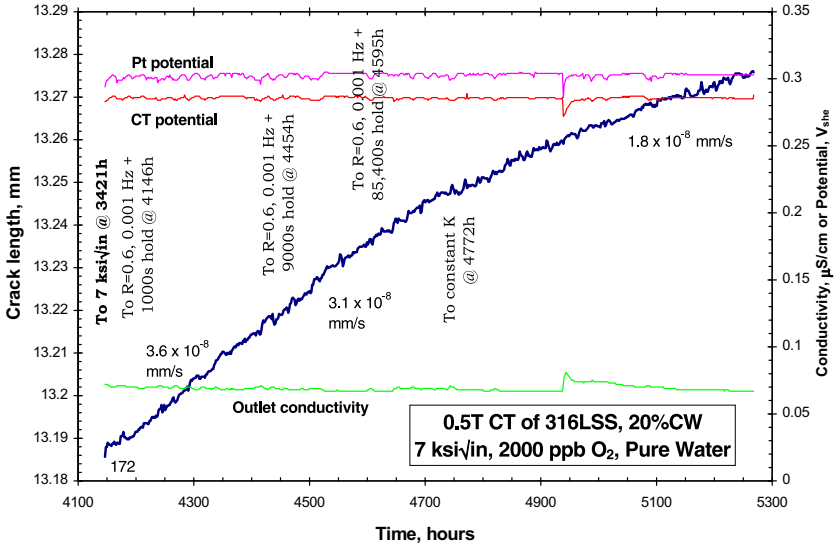

Fig. 6. Crack length vs. time for a 0.5TCT specimen of unsensitized Type 316L stainless steel 'cool' worked at +140 °C to 20% reduction in area.

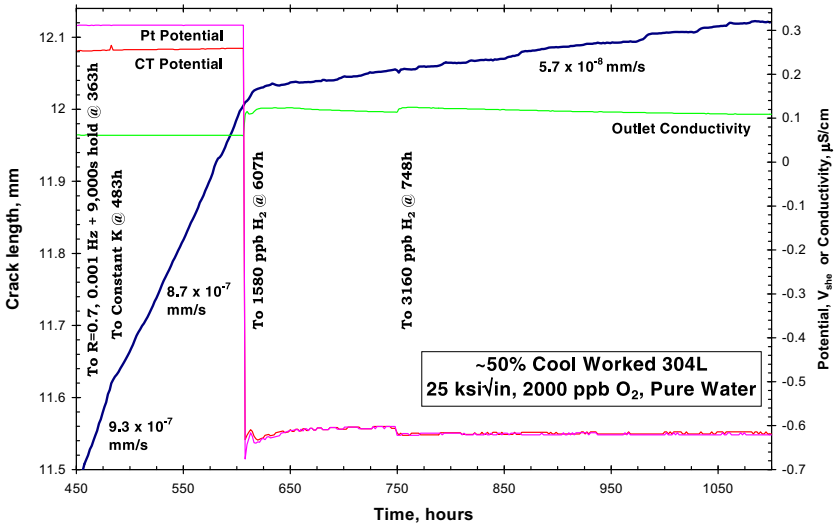

Fig. 7. Crack length vs. time for a 0.5TCT specimen of unsensitized Type 304L stainless steel 'cool' worked to ≈50% reduction in area.

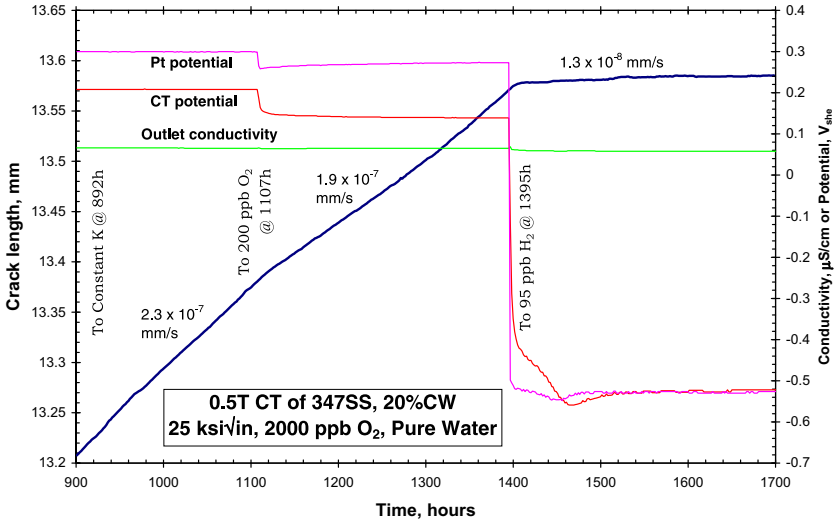

Fig. 8. Crack length vs. time for a 0.5TCT specimen of unsensitized Type 347L stainless steel 'cool' worked to ≈20% reduction in area.

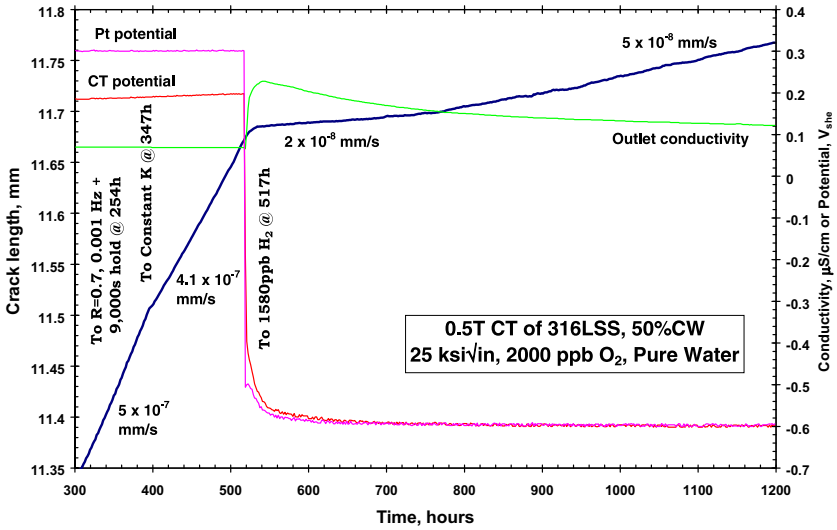

Fig. 9. Crack length vs. time for a 0.5TCT specimen of unsensitized Type 316L stainless steel 'cool' worked at +140 °C to 50% reduction in area.

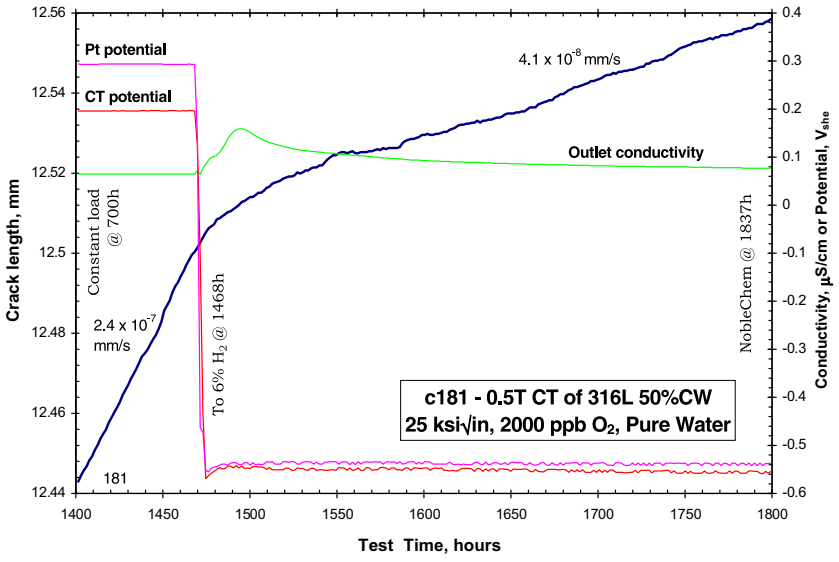

Fig. 10. Crack length vs. time for a 0.5TCT specimen of unsensitized Type 316L stainless steel 'cool' worked to ≈50% reduction in area.

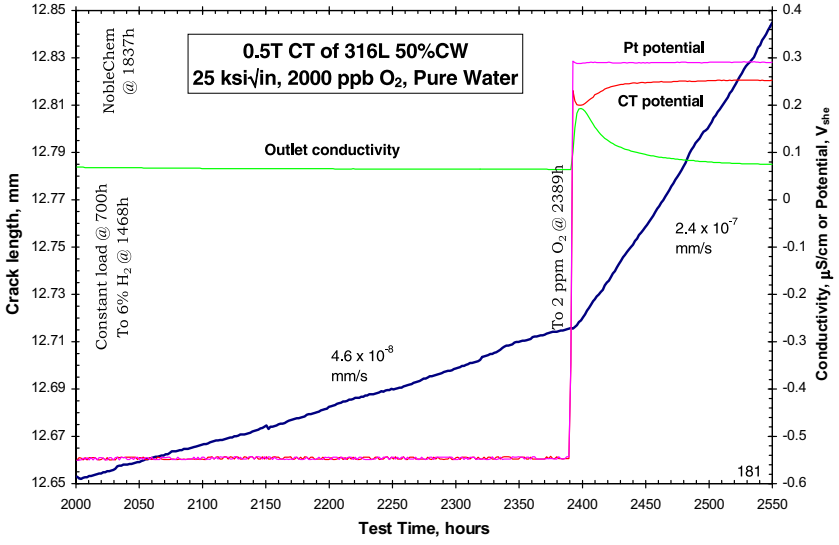

Fig. 11. Crack length vs. time for a 0.5TCT specimen of unsensitized Type 316L stainless steel 'cool' worked to ≈50% reduction in area.

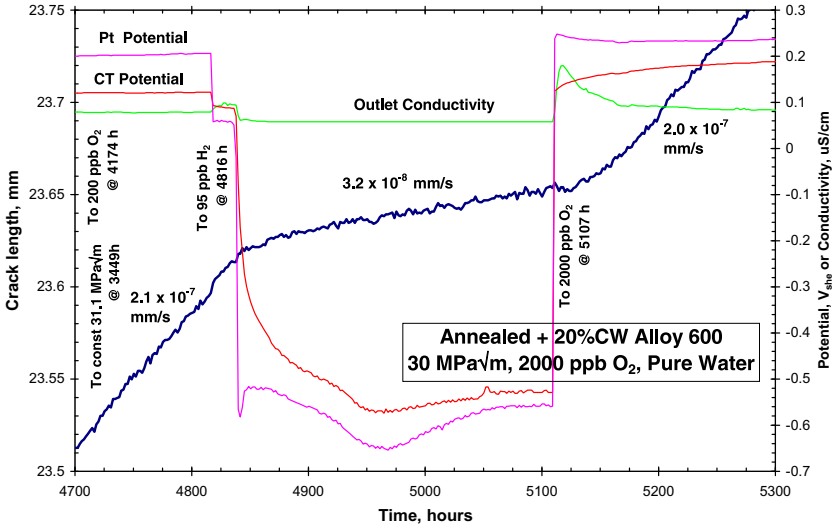

Fig. 12. Crack length vs. time for a 1TCT specimen of unsensitized alloy 600 cold worked at 25 °C to 20% reduction in area.

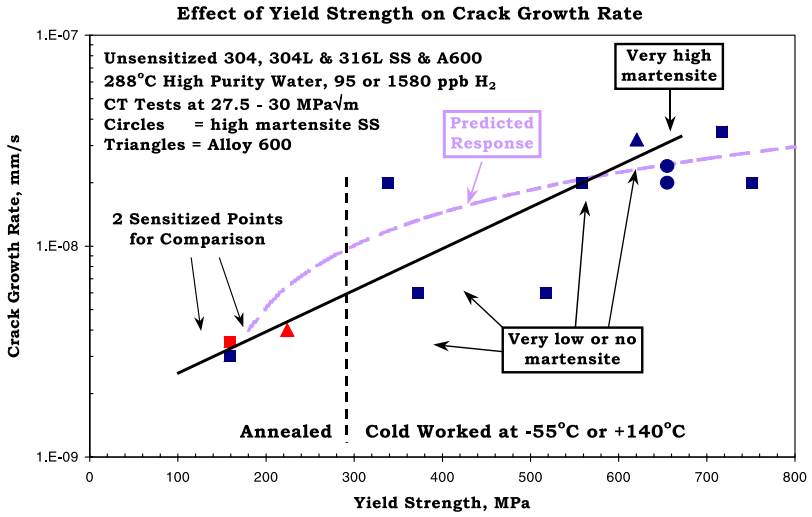

Fig. 13. Effect of yield strength and martensite on the stress corrosion crack growth rate on stainless steel and alloy 600 in 288 °C, high purity water (≈0.06 μS/cm outlet) containing 95 or 1580 ppb H_2.

288 °C water. Fig. 1(b) and (c) show the data from the SKI/EPRI round robin [18] (the smaller symbols at about +150 to +200 mV_{she}); Fig. 1(b) also includes data (larger symbols) under carefully controlled changes in potential and at low potential.

Usensitized (annealed) stainless steel is not immune to SCC (Figs. 1(c) and 2), even in ultra high purity H_2-deaerated water – rather, significant care must be used transitioning from a transgranular fatigue crack to intergranular SCC. Because some expressed concern for the role of prior exposure to O_2-containing water, some tests were conducted with exposure only to ultra high purity H_2-deaerated water; Figs. 3 and 4 shows that the SCC growth rates were not influenced by prior exposure to oxygenated water. Cracks in all cases are intergranular (Fig. 5) [15–17,19–21]. Many grades of unsensitized stainless steels have been shown to be susceptible to SCC, even in theoretical purity deaerated water. Thus, there can be no meaning to a *threshold* in *sensitization, neutron fluence, water purity, corrosion potential,* etc. Disproving that a threshold stress intensity factor, K (K_{ISCC}) exists is impossible, because everyone agrees that cracks won't grow at zero, but probing, e.g., below 1 ksi$\sqrt{}$in will likely forever remain impractical. However, the number of real cracks that grow from smooth surfaces (without the aid of pitting or other detectable cracking precursor) increases daily, and they must traverse the low K regime. Recent crack growth data for unsensitized stainless steel at 10 ksi$\sqrt{}$in and 7 ksi$\sqrt{}$in showed that stable crack growth at constant K was readily obtained (Fig. 6).

The difficulty in producing and measuring SCC growth in unsensitized stainless steels in deaerated water at many laboratories highlights the importance of testing techniques. A critical aspect of SCC testing is the transition from the transgranular fatigue pre-crack to intergranular SCC, although there are many other important testing controls and techniques [22]. The net result is the ability to reproducibly and accurately measure SCC growth rates under a wide variety of conditions, even at quite low rates. Reproducibility is a key consideration, and returning to identical test conditions to establish similar rates is an important measure of data quality (Fig. 2). Transitioning from transgranular fatigue to intergranular SCC is always easier at high crack growth rate, e.g., at high corrosion potential, but it is both possible and essential under any test condition.

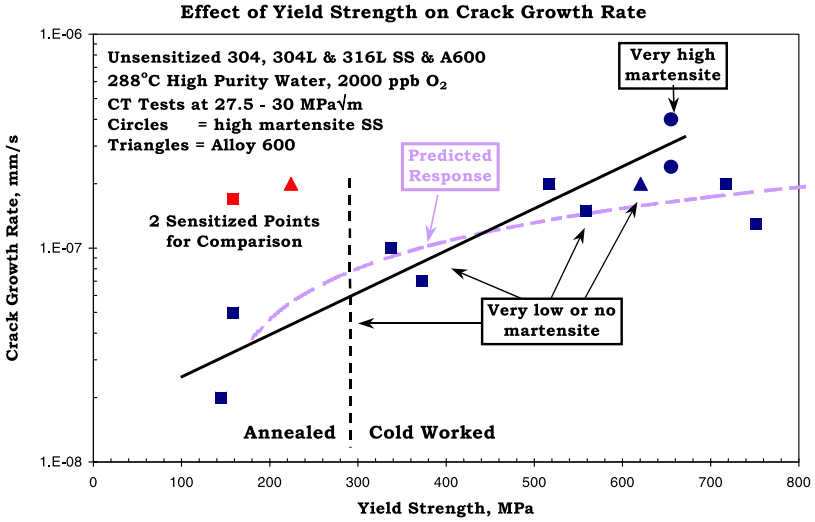

Fig. 14. Effect of yield strength and martensite on the stress corrosion crack growth rate on stainless steel and alloy 600 in 288 °C, high purity water (<0.10 μS/cm outlet) containing 2000 ppb O_2.

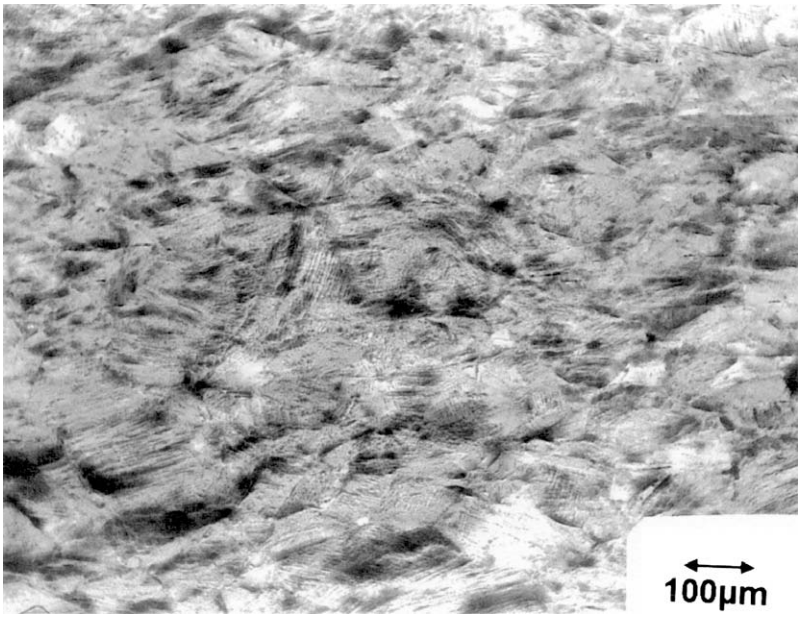

Fig. 15. Metallographic cross-section of Type 304L SS cross-rolled by 20% reduction in area at −55 °C.

All grades of stainless steel (304/304L/316/316L/321/347) show similar SCC growth rate response (Figs. 2 and 6–11). Indeed, the response of alloy 600 cold worked to a similar yield strength is identical to stainless steel (Fig. 12). For a given condition (i.e. yield strength, sensitization, etc.), the response of all 18-8 stainless steels is indistinguishable at low and high corrosion potential. As problematical as sensitization in stainless steel has been, an increase in yield strength to about 400 MPa is adequate to induce similar growth rates in unsensitized stainless steel (Fig. 1). The yield strength effect on growth rate at low and high potential is shown in Figs. 13 and 14.

There have long been concerns (based primarily on lower temperature (<150 °C) data) for the effects of martensite in stainless steel. To evaluate its effect, some stainless steels were worked at 140–240 °C to minimize or eliminate martensite, while others were worked at −55 °C where *very high* levels of martensite can form. At high cold reduction levels, the martensite levels, e.g., in Fig. 15 are so high (≈50%) that the material is strongly magnetic. However, as shown in Figs. 13 and 14, there is no consequential difference in crack growth rate at a given yield strength whether martensite is present or not – including in alloy 600 where martensite does not form.

To further evaluate the role of H_2, H_2 permeation was studied in stainless steel and alloy 600 at 288–340 °C [17,20,21,23–25]. The salient observations (Figs. 16 and 17) are that H_2 permeation is controlled by the coolant H_2 fugacity, which is non-zero even in water containing no H_2. The reproducibility of the data was excellent, even when repeats occurred a thousand hours later (Fig. 16). Once H_2 had permeated into the 4.6 mm ID tube, reducing the coolant fugacity readily produced dissociation of H_2 and permeation back into the coolant. Because the H_2 permeation rate is very high compared to the H_2 generation rate from corrosion, radiolytic proton injection, or transmutation, it is simply not possible to generate high H_2 fugacity in the metal. The measurements of high

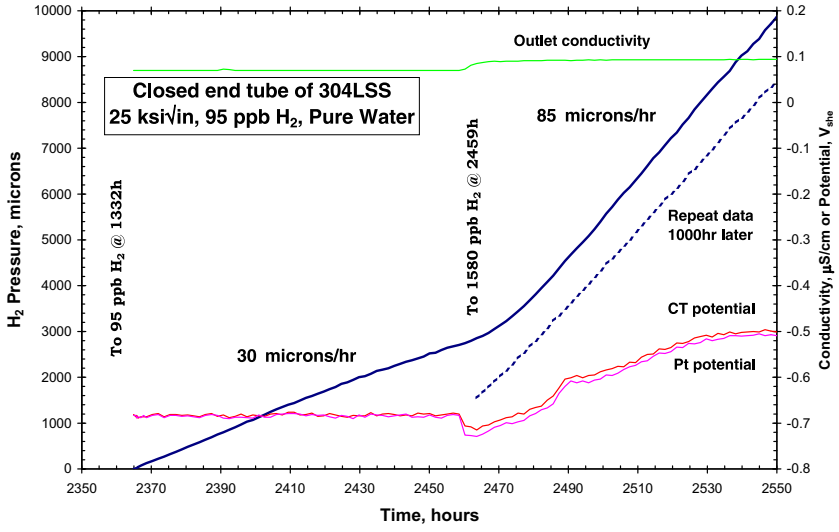

Fig. 16. Hydrogen permeation vs. time and coolant H_2 fugacity unsensitized Type 304L stainless steel.

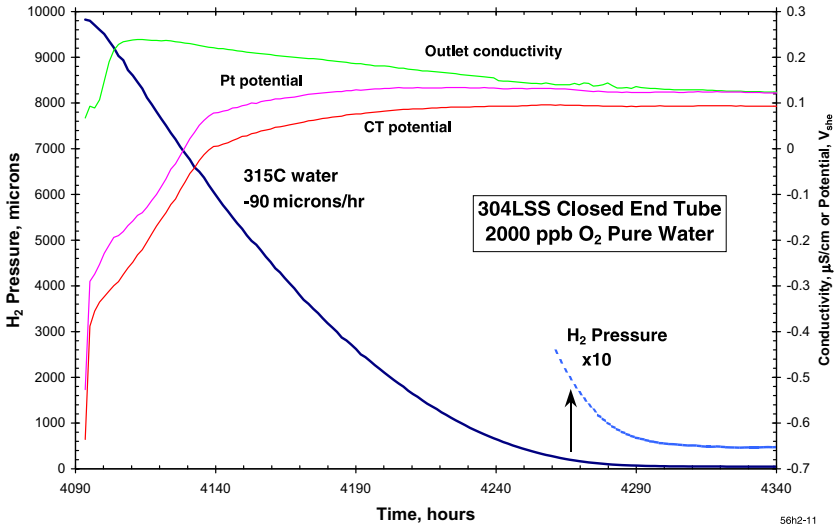

Fig. 17. Hydrogen permeation vs. time and coolant H_2 fugacity unsensitized Type 304L SS.

hydrogen concentration in metals [26,27] is simply a reflection of hydrogen storage locations, e.g., at radiation-induced voids – not of a high hydrogen fugacity that can have extraordinary effects on the microstructure. Evaluation of the effects of H_2 in deaerated water shows no difference in growth rate on changing from N_2 deaerated water to various levels of H_2 (e.g. Fig. 18). Similarly, the effect of electrocatalytic species (e.g. Pt) on the surface has no accelerating effect on the crack growth rate in deaerated water.

The role of H_3BO_3 and LiOH (or HN_3) on SCC in deaerated water is considered to be minimal [9], because they only shift the pH from 5.63 (for 288 °C pure water) to 6.7 to 7.6 (depending on the balance of B and Li used). This is reflected in the crack growth rate response shown in Fig. 19 for stainless steel and Alloy 600. However, just because it has the capacity to pH buffer does not mean that it's an innocuous impurity when thermal or potential gradients exist in the crack, as shown in Fig. 20.

The response of a model alloy of stainless steel containing 5% Si (Fe–15Ni–12Cr–5Si–1Mn–0.033C) and cool worked to 22% reduction in area is shown in Fig. 21. This elevated level of grain boundary Si is designed to address the possible role of high grain boundary Si from radiation segregation. After pre-cracking, this material exhibited very high growth rates, and transitioned to constant *K* conditions very readily. At 312 h, the water chemistry was changed from 2000 ppb O_2 to 95 ppb H_2, with the appropriate decrease in corrosion potential of the CT specimen observed. However, there was no discernable effect on the crack growth rate. Indeed, toward the end of the test, a decreasing K profile was applied which dropped the *K* from 27 ksi$\sqrt{}$in to 10 ksi$\sqrt{}$in – only a limited effect on crack growth rate was observed. The absence of typical dependencies on corrosion potential and stress intensity suggests that the crack may be advancing by an altered mechanism, most likely direct dissolution of grain boundary silicon. However, this may reflect a high level of grain boundary silicon segregation in this unusual 5% Si alloy.

It should be noted that such *bulk* model alloys provide a very limited window into the behavior of alloys that have only very localized grain boundary segregation (in radiation segregation, the composition profile is limited to a few nm). This is partly be-

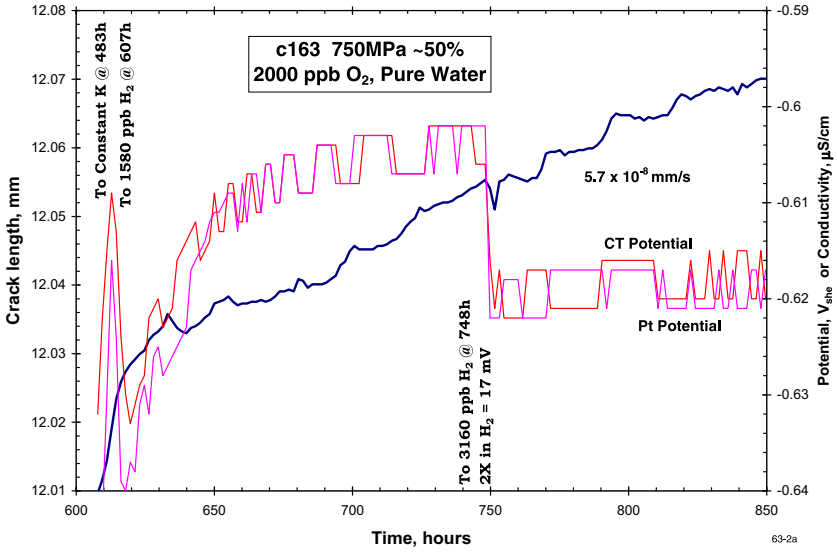

Fig. 18. Crack length vs. time for a 0.5TCT specimen of unsensitized Type 304L stainless steel 'cool' worked to ≈50% reduction in area.

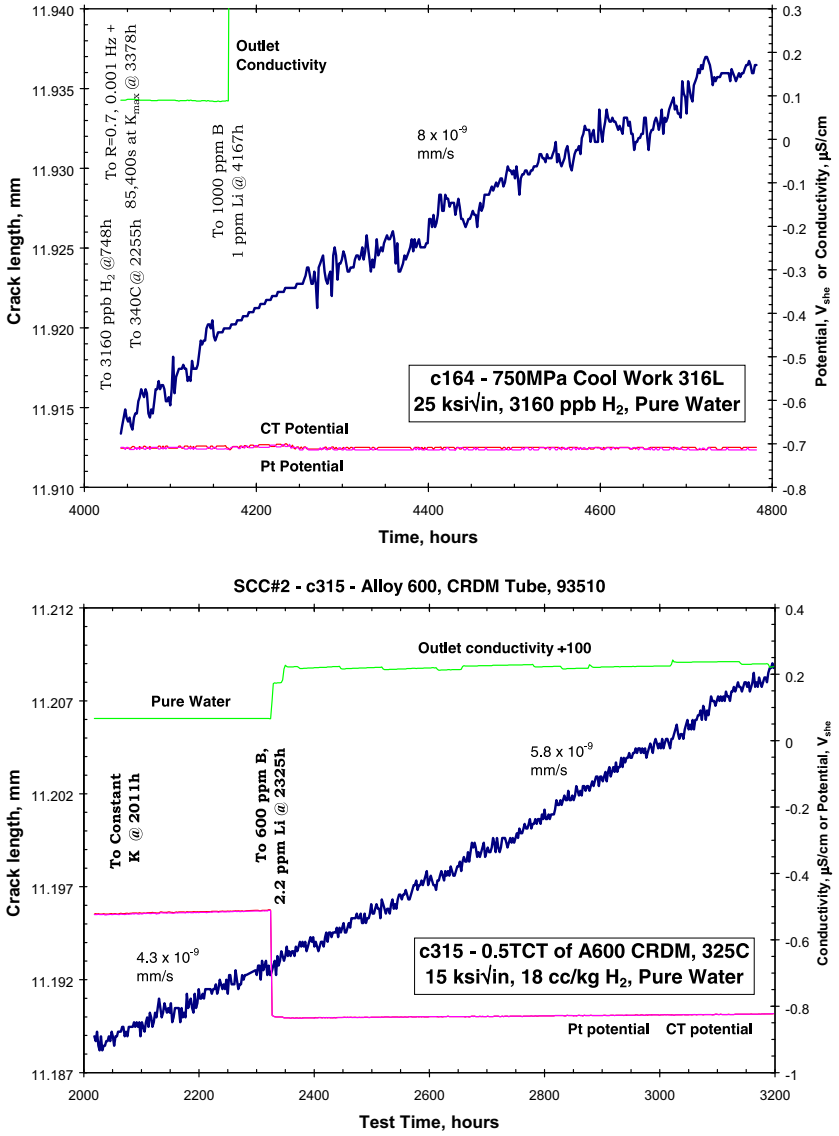

Fig. 19. Crack length vs. time for a 0.5TCT specimen tested in deaerated water as B/Li were added. Top: unsensitized Type 316L stainless steel with 50% cold work. Bottom: annealed alloy 600.

cause the compositional changes affect bulk properties, and if there is any clear lesson from the work on cold worked stainless steel, it is that the bulk (i.e. not specifically the crack tip) characteristics play an important role, presumably through the mechanics of the crack tip deformation rate. This comment is reinforced by the observation that high purity (very low Si) stainless steels routinely show greater susceptibility to SCC following irradiation than normal stainless steels [26,28].

High yield strength materials (high cold work, irradiation, etc.) can exhibit both high growth rates and a more limited effect of corrosion potential at high stress intensity factor or under cyclic loading conditions (even under 'gentle' cyclic loading conditions (Fig. 22), which typically enhance the SCC growth rate only very slightly). However, in some high yield strength materials, rapid crack advance is observed during the reloading portion of the waveform, which translates to rates during that time period of 10^{-4} mm/s. Whether this 'gentle' cyclic phenomenon at $R = s0.7$ would be observed under higher frequency, lower amplitude conditions needs to be evaluated. High growth rates are also observed as the stress intensity increases at constant K. Fig. 23 shows the very high growth rates and, while there is some reduction as the corrosion potential is decreased, the rate rapidly increases as the crack depth and stress intensity increases.

Elevated yield strength can result from bulk cold work, surface cold work, precipitation hardening, radiation hardening, and shrinkage strains in weld heat affected zones. Of these, perhaps the least recognized until recently is weld shrinkage strains. Historically, the primary concerns for welding have revolved around weld sensitization and weld residual stresses. Recently, a new technique has been developed to more precisely and locally measure weld residual strains [19,29,30], and it shows that the peak strains are close to the weld fusion line and typically range from 8% to 20% equivalent room temperature strain (the amount of strain that actually occurs during weld solidification and cooling is higher and impossible to measure after the fact because of self-annealing – thus, we use a 'equivalent room temperature strain' to capture the residual effect). Figs. 24 and 25 are examples of the SCC response in 304L, 316L and 347L stainless steels, where SCC occurs in the heat affected zone. These measurements are complex because regions of the weld where the fusion line is fairly

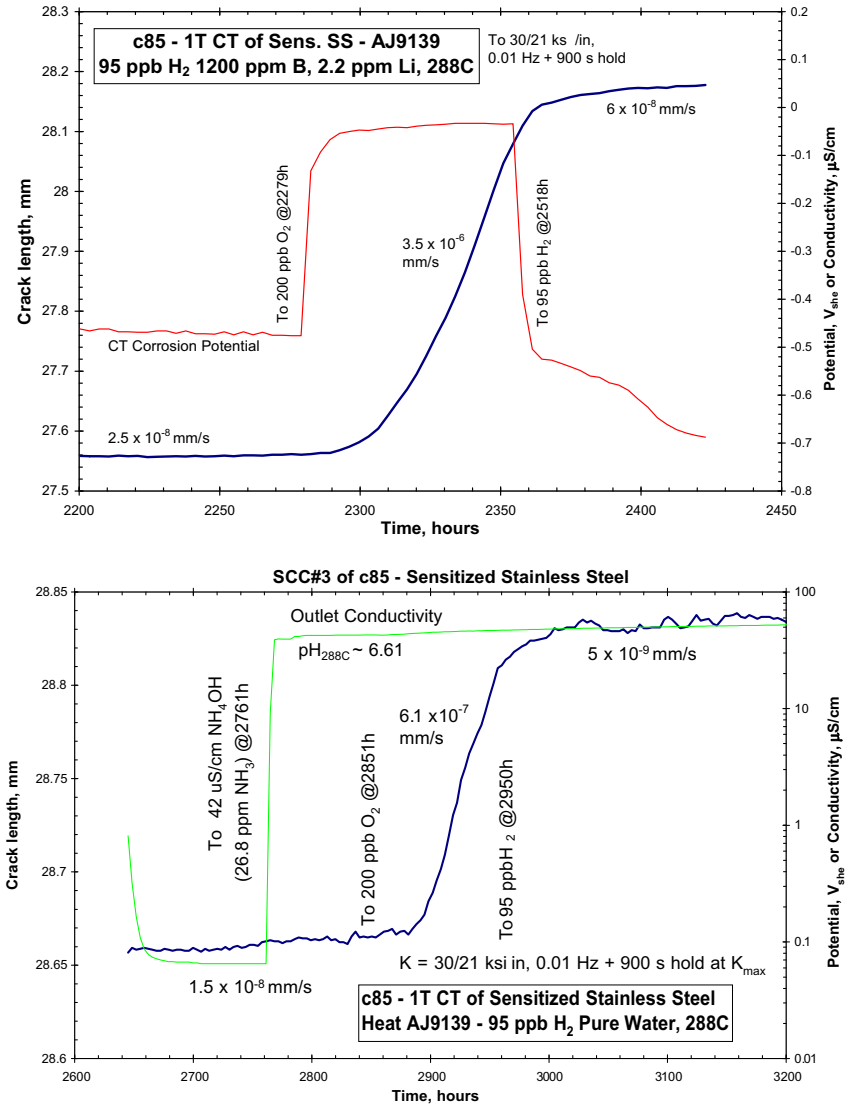

Fig. 20. Crack length vs. time for a 0.5TCT specimen of unsensitized Type 304L stainless steel 'cool' worked to ≈50% reduction in area tested in aerated water with B/Li additions (top) or HN_3 additions (bottom).

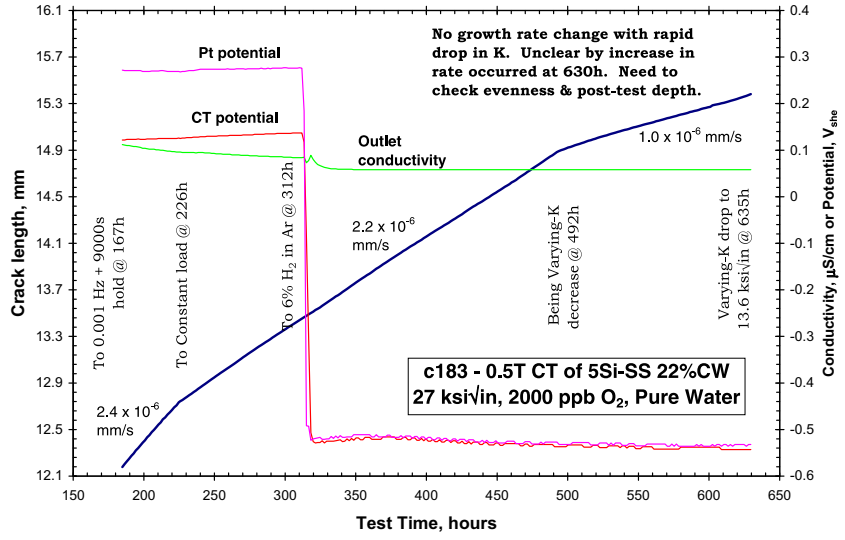

Fig. 21. Crack length vs. time for a 0.5TCT specimen of an unsensitized model 'stainless steel' containing 5% Si 'cool' worked to 22% reduction in area.

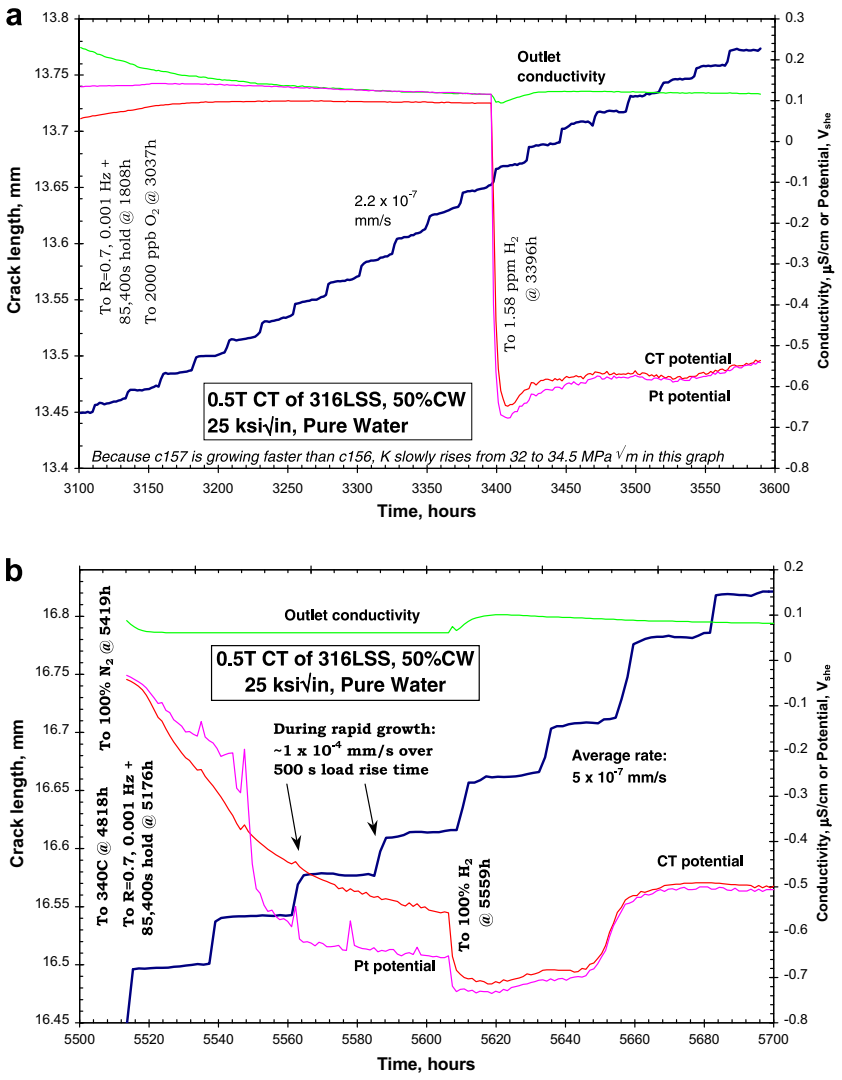

Fig. 22. (a, b). Crack length vs. time for a 0.5TCT specimen of an unsensitized 316L stainless steel 'cool' worked to 50% showing the effect of gentle unloading cycles on environmental crack advance on stainless steel whose yield strength is elevated by cold work.

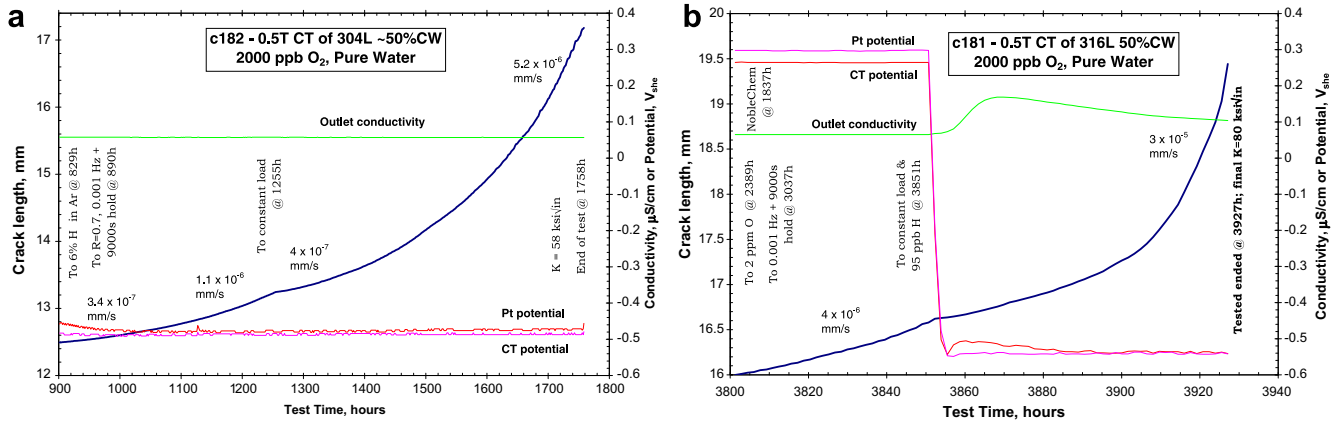

Fig. 23. (a, b). Crack length vs. time for 0.5TCT specimens of an unsensitized Types 304L and 316L stainless steel 'cool' worked to 50% showing the effect of high yield strength and high stress intensity on environmental crack advance and fracture toughness.

straight must be identified, then the material polished and etched on both sides, then the CT specimen precisely aligned and machined so that the plane of cracking is optimally oriented. These rates are generally lower than those observed on 20–50% cold worked stainless steel, entirely consistent with their lower (<20%) residual strain levels.

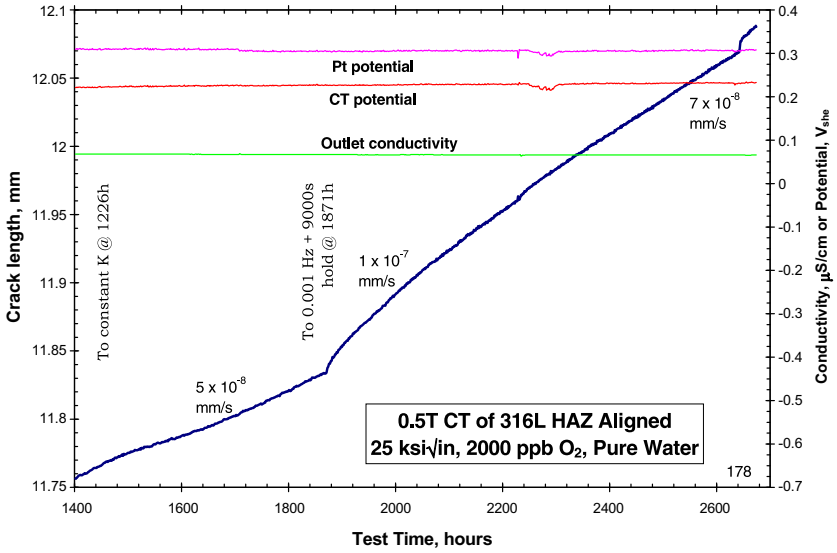

Fig. 24. Crack length vs. time for a weld HAZ aligned 0.5TCT specimen of unsensitized Type 316L SS.

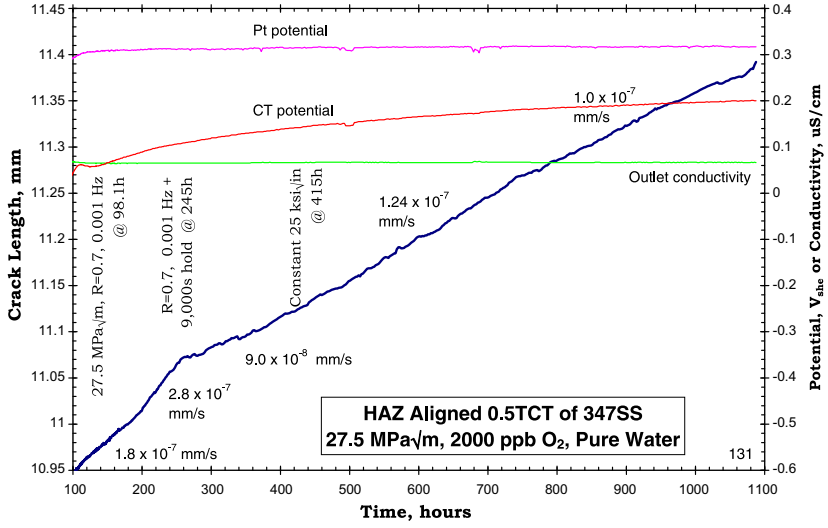

Fig. 25. Crack length vs. time for a weld HAZ aligned 0.5TCT specimen of unsensitized Type 347 SS.

It is interesting to note that the historical inattention to weld residual strain in sensitized stainless steel piping is not inconsistent with the phenomenon. That is, the peak in sensitization in 304/316 stainless steel does not occur near the weld fusion line, but typically 5–10 mm away where the thermal profiles favor nucleation and growth of grain boundary carbides. Similarly, the peak in weld residual stress is also typically 2–5 mm away from the fusion, although this is more sensitive to the welding technique. At the 5–10 mm distance, the role of residual strain is much less pronounced, and ignoring its contribution represents a small oversight. As SCC has developed in unsensitized stainless steel weld heat affected zones, the role of residual strain is much more important, and indeed most cracks are observed to occur close to the weld fusion line. The reason why unsensitized stainless steel piping (e.g. 304L/316NG) shows so little SCC, while unsensitized stainless steel shrouds show a significant incidence is that the corrosion potential is higher (other factors also differentiate pipe welds from shroud welds).

Cold worked vs. irradiated stainless steel exhibit similar response at a given yield strength [31], which may seem surprising given the very different nature of the microstructure and hardening mechanism. However, the effect of yield stress appears to be to constrain the size of the plastic zone to smaller dimensions at a given stress intensity, which gives rise to steeper strain gradients near the crack tip [21,31]. It is interesting to note that recent studies on alloy X750 showed high growth rates under both high and low corrosion potential conditions (Fig. 26).

The predicted response (by PLEDGE) of yield strength, corrosion potential, and sensitization effects is shown in Figs. 1, 13 and 14. The prediction concepts, algorithms, and numerical values are almost totally unchanged in the ~25 years since they were formulated (e.g. for the effects of corrosion potential, sensitization, stress intensity, water purity/specific anion concentrations, etc.), with the effects of yield strength from cold work and irradiation (as well as other irradiation effects) incorporated 20 years ago.

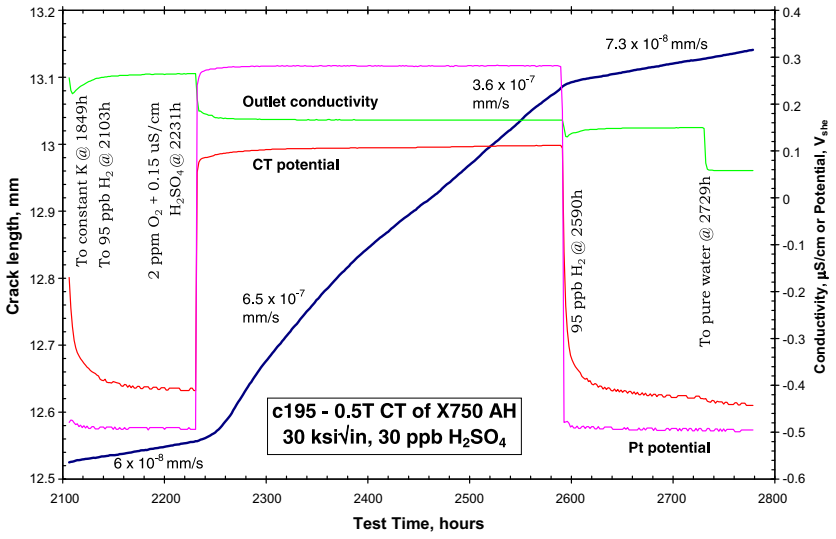

Fig. 26. Crack length vs. time for a 0.5TCT specimen of alloy X750.

4. Conclusions

SCC growth rates were evaluated on unsensitized stainless steels and nickel alloys in high temperature, (usually) ultra high purity water. SCC was strongly affected by yield strength, corrosion potential, and temperature, and was essentially independent of the martensite content per se, the type and heat of material, the hydrogen fugacity, and the hydrogen permeation rate (which was controlled by the H_2 fugacity in the coolant). These observations are inconsistent with a hydrogen-controlled mechanism of crack advance. The behavior of various grades of stainless steel (and alloy 600) at 20% cold work were essentially identical at both low and high corrosion potential.

The importance of weld residual strain was confirmed using HAZ aligned CT specimens, which showed significant SCC susceptibility, although the rates were somewhat lower than those measured in specimens with 20–50% bulk cold work, consistent with the lower residual strain in the HAZ (on average) and with the challenge of finding a planar weld fusion line in which to locate the crack plane. Unusually high SCC growth rates were observed in a model stainless steel containing 5% Si, and in high yield strength stainless steels tested at high stress intensity and/or under cyclic loading conditions. The SCC response at a similar yield strength was similar for cold worked and irradiated materials tested at low potential (where radiation induced Cr depletion plays a minimal role). The PLEDGE model accurately predicts the effect on SCC growth rates of yield strength, corrosion potential, alloy type/heat, sensitization, and other factors.

References

[1] F.P. Ford, P.L. Andresen, in: P. Marcus, J. Ouder (Eds.), Corrosion Mechanisms, Marcel Dekker, 1994, p. 501.
[2] P.L. Andresen, F.P. Ford, Mater. Sci. Eng. A103 (1988) 167.
[3] F.P. Ford, D.F. Taylor, P.L. Andresen, R.G. Ballinger, Corrosion Assisted Cracking of Stainless and Low Alloy Steels in LWR Environments, EPRI Contract RP2006-6, Report NP5064M, February 1987.
[4] P.L. Andresen, Conceptual Similarities and Common Predictive Approaches for SCC in High Temperature Water Systems, Paper 96258, Corrosion/96, NACE, 1996.
[5] P.L. Andresen, F.P. Ford, S.M. Murphy, J.M. Perks, State of knowledge of radiation effects on environmental cracking in light water reactor core materials, in: Proceedings of the 4th International Symposium on Environmental Degradation of Materials in Nuclear Power Systems – Water Reactors, NACE, 1990, p. 1-83.
[6] P.L. Andresen, L.M. Young, Characterization of the roles of electrochemistry, convection and crack chemistry in stress corrosion cracking, in: Proceedings of the 7th International Symposium on Environmental Degradation of Materials in Nuclear Power Systems – Water Reactors, NACE, 1995, p. 579.
[7] P.L. Andresen, F.P. Ford, Corros. Sci. 38 (1996) 1011.
[8] G.R. Engelhardt, D.D. Macdonald, M. Urquidi-Macdonald, Corros. Sci. 41 (1999) 2267. see p. 2288.
[9] P.L. Andresen, P.W. Emigh, M.M. Morra, J. Hickling, Effects of PWR primary water chemistry and deaerated water on SCC, in: Proceedings of the 12th International Symposium on Environmental Degradation of Materials in Nuclear Power Systems – Water Reactors, TMS, Snowbird, August 2005.
[10] P.L. Andresen, C.L. Briant, Corrosion 45 (1989) 448.
[11] P.L. Andresen, C.L. Briant, Role of S, P and N segregation on intergranular environmental cracking of stainless steels in high temperature water, in: Proceedings of the 3rd International Symposium on Environmental Degradation of Materials in Nuclear Power Systems – Water Reactors, AIME, 1988, p. 371.
[12] P.L. Andresen, Corrosion 44 (7) (1988) 450.
[13] P.L. Andresen, The Effects of Aqueous Impurities on Intergranular Stress Corrosion Cracking of Sensitized Type 304 Stainless Steel, Final Report NP3384 Contract T115-3, EPRI, 1983. See also, 'Innovations in Experimental Techniques for Testing in High Temperature Aqueous Environments', Report No. 81CRD088, GE CRD, Schenectady, New York, 1981.
[14] L.W. Niedrach, J. Electrochem. Soc. 127 (1980) 2122.
[15] P.L. Andresen, T.M. Angeliu, L.M. Young, Immunity, thresholds, and other SCC fiction, in: Proceedings of the Staehle Symposium on Chemistry and Electrochemistry of Corrosion and SCC, TMS, February 2001.
[16] P.L. Andresen, Perspective and direction of stress corrosion cracking in hot water, in: Proceedings of the Tenth International Symposium on Environmental Degradation of Materials in Nuclear Power Systems - Water Reactors, NACE, 2001.
[17] P.L. Andresen, T.M. Angeliu, L.M. Young, W.R. Catlin, R.M. Horn, Mechanisms and kinetics of SCC in stainless steels, in: Proceedings of the Tenth International Symposium on Environmental Degradation of Materials in Nuclear Power Systems – Water Reactors, NACE, 2001.
[18] P.L. Andresen, K. Gott, J.L. Nelson, Stress corrosion cracking of sensitized Type 304 stainless steel in 288C water: A five laboratory round Robin, in: Proceedings of the Ninth International Symposium on Environmental Degradation of Materials in Nuclear Power Systems – Water Reactors, AIME, 1999.
[19] P.L. Andresen, T.M. Angeliu, W.R. Catlin, L.M. Young, R.M. Horn, Effect of Deformation on SCC of Unsensitized Stainless Steel, Corrosion/2000, Paper 00203, NACE, 2000.
[20] P.L. Andresen, T.M. Angeliu, L.M. Young, Effect of Martensite & Hydrogen on SCC of Stainless Steels, Paper #01228, Corrosion/01, NACE, 2001.
[21] P.L. Andresen, L.M. Young, P.W. Emigh, R.M. Horn, Stress Corrosion Crack Growth Rate Behavior of Ni Alloys 182 and 600 in High Temperature Water, Corrosion/02, Paper 02510, NACE, 2002.
[22] P.L. Andresen, SCC testing and data quality considerations, in: Proceedings of the Ninth International Symposium on Environmental Degradation of Materials in Nuclear Power Systems – Water Reactors, AIME, 1999. See also, P.L. Andresen, 'Experimental Quality Guidelines for SCC Testing', GE CRD, January 30, 1998.
[23] D.S. Morton, S.A. Attanasio, J.S. Fish, M.K. Schurman, Influence of Dissolved Hydrogen on Nickel Alloy SCC in High Temperature Water, Corrosion/99, Paper 99447, NACE, 1999.

[24] D.S. Morton, S.A. Attanasio, G.A. Young, P.L. Andresen, T.M. Angeliu, The Influence of Dissolved Hydrogen on Nickel Alloy SCC: A Window to Fundamental Insight, Corrosion, Paper 01117, NACE, 2001.
[25] P.L. Andresen, unpublished data on H_2 permeation in alloy 600 and stainless steel, April 2001.
[26] P.L. Andresen, in: R.H. Jones (Ed.), Book on Stress Corrosion Cracking: Materials Performance and Evaluation, ASM, 1992, p. 181.
[27] A.J. Jacobs, Hydrogen buildup in irradiated Type 304 stainless steel, in: F.A. Garner, N.H. Packan, A.S. Kumar (Eds.), Proceedings of the 13th Symposium Radiation Induced Changes in Microstructure, STP 956, vol. II, ASTM, Phila., 1985, p. 239.
[28] T.M. Karlsen, E. Hauso, Qualification and application of instrumented specimens for in-core studies on cracking behavior or austenitic stainless steels, in: Proceedings of the Ninth International Symposium on Environmental Degradation of Materials in Nuclear Power Systems – Water Reactors, AIME, 1999, p. 951.
[29] T.M. Angeliu, P.L. Andresen, J.A. Sutliff, R.M. Horn, Intergranular stress corrosion cracking of unsensitized stainless steels in BWR environments, in: Proceedings of the Ninth International Symposium on Environmental Degradation of Materials in Nuclear Power Systems – Water Reactors, AIME, 1999, p. 311.
[30] T.M. Angeliu, P.L. Andresen, E. Hall, J.A. Sutliff, S. Sitzman, Strain and Microstructure Characterization of Austenitic Stainless Steel Weld HAZs, Corrosion/2000, Paper 00186, NACE, 2000.
[31] P.L. Andresen, Similarity of Cold Work and Radiation Hardening in Enhancing Yield Strength and SCC Growth of Stainless Steel in Hot Water, Corrosion/02, Paper 02509, NACE, 2002.